

Bayesian inference of mixed Gaussian phylogenetic models

Bayu Brahmantio^{1*}, Krzysztof Bartoszek¹ and Etká Yapar²

¹Department of Computer and Information Science, Linköping
University, Sweden.

²Department of Biology, Lund University, Sweden.

*Corresponding author(s). E-mail(s): bayu.brahmantio@liu.se;
Contributing authors: krzysztof.bartoszek@liu.se; etka.yapar@biol.lu.se;

Abstract

Background: Continuous traits evolution of a group of taxa that are correlated through a phylogenetic tree is commonly modelled using parametric stochastic differential equations to represent deterministic change of trait through time, while incorporating noises that represent different unobservable evolutionary pressures. Often times, a heterogeneous Gaussian process that consists of multiple parametric sub-processes is often used when the observed data come from a very diverse set of taxa. In the maximum likelihood setting, challenges can be found when exploring the involved likelihood surface and when interpreting the uncertainty around the parameters.

Results: We extend the methods to tackle inference problems for mixed Gaussian phylogenetic models (MGPMs) by implementing a Bayesian scheme that can take into account biologically relevant priors. The posterior inference method is based on the Population Monte Carlo (PMC) algorithm that are easily parallelized, and using an efficient algorithm to calculate the likelihood of phylogenetically correlated observations. A model evaluation method that is based on the proximity of the posterior predictive distribution to the observed data is also implemented. Simulation study is done to test the inference and evaluation capability of the method. Finally, we test our method on a real-world dataset.

Conclusion: We implement the method in the R package `bgphy`, available at github.com/bayubeta/bgphy. Simulation study demonstrates that the method is able to infer parameters and evaluate models properly, while its implementation on the real-world dataset indicates that a carefully selected model of evolution based on naturally occurring classifications results in a better fit to the observed data.

Keywords: Phylogenetic comparative methods, Bayesian statistics, evolution, Gaussian diffusion process

1 Background

The study of between-species phenotypic data requires taking into consideration the evolutionary dependency structure between them. Approaches for this have been developed from the second-half of the previous century (see, e.g., [1] and [2]). The current widespread availability of computational power and genetically derived phylogenies allowed for an extraordinary growth in numbers of models and software for this field termed phylogenetic comparative methods (PCMs). The high-level framework is that of a branching Markov process, with different processes and parameters corresponding to different biological hypotheses about the evolution of considered traits. However, the majority of contemporary software assumes that the model is homogeneous over the phylogeny, with perhaps some particular parameter being allowed to vary. This is despite evolutionary relationships spanning through millions of years through varying environments. To (at least partially) remedy this the mixed Gaussian phylogenetic models (MGPMs) framework was introduced [3].

In the MGPM approach, the tree is partitioned into multiple disjoint components (called regimes). Inside each component, the trait(s) evolve under some model from the so-called \mathcal{G}_{LInv} family [4]. An illustration on how the evolutionary processes happen using this framework can be seen on Figure 1. Under this family the transition density of the trait along a time interval is Gaussian with expectation depending linearly on the ancestral value and a variance that is invariant with respect to the ancestral value. The phylogenetic Brownian motion (BM) and Ornstein-Uhlenbeck (OU) processes, which are the current work-horses of PCMs, are part of this family. Importantly for the inference, this MGPM framework allows for linear in time with respect to the number of tips on the tree likelihood evaluation [4].

The majority of parameter inference techniques for PCMs are maximum likelihood ones, with competing hypotheses concerning the evolutionary history (models, constraints on parameters, regimes on phylogeny configuration) compared using some information criterion. Another view of the statistical modelling is to utilize Bayesian methods to infer the posterior distribution of evolutionary parameters given the data.

In this work, we enhance the framework of MGPMs by implementing a Bayesian inference method for the combinations of univariate BM and OU processes on the phylogeny. We apply a Monte Carlo method that is based on importance sampling technique for simulating from the posterior distribution of the model's parameters. Furthermore, we implement a model evaluation method that takes into account the proximity between the empirical distribution and the posterior predictive distribution.

The rest of the paper is organized as follows. We start by explaining the notations and theoretical background needed for the rest of the paper. In the following subsection, we discuss about Bayesian approach to MGPMs. We proceed by describing our method to simulate the posterior distribution of MGPM parameters. We then explain

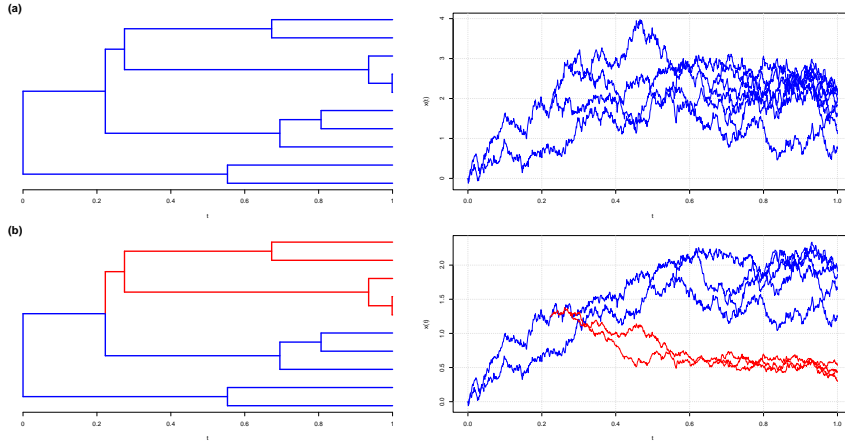


Fig. 1 An illustration of MGPMs on a simple phylogenetic tree. The right column shows simulated processes that follow the phylogenetic tree on the left. In (a), a homogeneous process is assumed throughout the whole tree. In (b), the tree is partitioned into the blue and red regimes, each with its own process. The evolution starts with the process in the blue regime at time $t = 0$, but one part of the tree switches to the process in the red regime at some point in time until $t = 1$.

the setup for simulation studies and implement our method into antlers dataset [5]. The results of the simulation studies and real-world dataset are discussed, as well as its limitations. We conclude our paper by discussing the outcomes and future improvements of our work.

1.1 Notations and theoretical background

Let \mathcal{T} be an ultrametric phylogenetic tree with n number of tips, hence $n - 1$ internal nodes. We assume that the tree is known and fixed, and the data can only be observed at the tips. Denote $\mathbf{x} = (x_1, x_2, \dots, x_n)^\top$ as the vector of measurements at the tips of the tree, i.e., x_i is the measurement on the taxa i , while $\mathbf{z} = (z_1, z_2, \dots, z_{n-1})^\top$ denotes the internal nodes. Furthermore, the set of branches (edges) of the tree \mathcal{T} can be written as $\mathbf{b}(\mathcal{T})$. Together, \mathbf{x} , \mathbf{z} , and $\mathbf{b}(\mathcal{T})$ completely determine the tree \mathcal{T} .

We assume a coloring of the branches $\mathbf{b}(\mathcal{T})$, which we will address as "regimes configuration", that results in K disjoint sets of $\mathbf{b}(\mathcal{T})$, addressed as "evolutionary regimes" or "regimes" shortly (see Figure 1(b), left panel, for $K = 2$). This setup also makes it possible for a regime to be disconnected across different parts of the tree.

Denote $\mathbf{M} = \{\mathcal{M}_i\}_{i=1}^K$ as the set of all models from all K regimes, with the corresponding parameters $\Theta = \{\Theta_i\}_{i=1}^K$. Assuming that all models are of the \mathcal{G}_{LInv} family, the transition probability under each model, given some ancestral value $x(s)$, $s < t$, is

$$\left(x(t) \mid x(s), \mathcal{M}_i, \Theta_i \right) \sim \mathcal{N} \left(x(t) \mid a_{l, \mathcal{M}_i, \Theta_i} x(s) + b_{l, \mathcal{M}_i, \Theta_i}, V_{l, \mathcal{M}_i, \Theta_i} \right), \quad (1)$$

where $l = t - s$, \mathcal{M}_i is the model type (BM or OU) for the regime i with parameters Θ_i , and a , b , and V are functions that depends on \mathcal{M}_i , Θ_i , and l . For example, if \mathcal{M}_1

is a BM process and \mathcal{M}_2 is an OU process, defined respectively as

$$dx(t) = \sigma_1 dW(t), \quad (2)$$

$$dx(t) = -\alpha_2(x(t) - \theta_2)dt + \sigma_2 dW(t), \quad (3)$$

we have $\Theta_1 = \sigma_1$ and $\Theta_2 = (\alpha_2, \theta_2, \sigma_2)^\top$. We can also set the ancestral value at the root of the tree, X_0 , as a free parameter. Hence, the full collection of parameters from a given MGPM with K regimes is $\Theta = (X_0, \Theta_1, \dots, \Theta_K)^\top = (X_0, \vartheta_{1,1}, \dots, \vartheta_{1,n_1}, \dots, \vartheta_{K,1}, \dots, \vartheta_{K,n_K})^\top$. Returning to the previous example, the full parameters of the previously-mentioned MGPM is $\Theta = (X_0, \sigma_1, \alpha_2, \theta_2, \sigma_2)^\top$.

1.2 Bayesian approach to MGPMs

Since all models, given an ancestral value $x(s)$, have Gaussian transition probabilities and further assuming that changes become independent after branching, x_i given X_0 will be Gaussian and moreover the joint density of \mathbf{x} will be multivariate normal by marginalizing over all the internal nodes. A procedure for calculating the likelihood, $\mathcal{L}(\Theta) = p(\mathbf{x}|\Theta)$, is implemented by marginalizing over all internal nodes of the tree in an efficient way through the so-called pruning algorithm.

In the maximum likelihood setting, the parameters Θ^* that maximizes the likelihood function $\mathcal{L}(\Theta)$ can then be searched given an MGPM. Additionally, we can calculate their information score, e.g., AIC and BIC, to choose between different hypothesized models.

Another perspective to tackle the parameter estimation and model evaluation problem is to use a Bayesian approach. As discussed in previous studies ([6], [7], [8]), a relevant prior distribution for the parameters helps in easing off identifiability issues that presents in the OU models, which is one of the models considered in this study. A prior distribution is also a natural way to safeguard the inference from unrealistic parameter values that could arise in the maximum likelihood setting, where the maximum search could stuck in a local optimum that does not always translate to a realistic parameter value. Furthermore, the posterior distribution offers an inherent probabilistic interpretation of uncertainty for the parameters.

Applying Bayes' theorem, the density function of the density function of the posterior distribution of the parameters of a given MGPM setup is

$$p(\Theta|\mathbf{x}) = \frac{p(\mathbf{x}|\Theta)p(\Theta)}{p(\mathbf{x})} \propto \mathcal{L}(\Theta)p(\Theta), \quad (4)$$

where the parameters are assumed to be pairwise independent in the prior, i.e.,

$$p(\Theta) = p(X_0) \prod_{i=1}^K p(\Theta_i) = p(X_0) \prod_{i=1}^K \prod_{j=1}^{n_K} p(\vartheta_{i,j}), \quad (5)$$

and we drop in the notation of the implicit dependence on the model \mathbf{M} and the tree \mathcal{T} . Hence, we can set the appropriate prior distribution for each parameter individually. The posterior distribution is in general not available in a closed-form formula.

Since we can still compute the likelihood and the prior density, we resort to an approximation procedure with Monte Carlo methods to calculate quantities of the posterior distribution.

This work differs from the previously done studies on Bayesian PCMs in different ways. In `bayou` [6], the regimes are considered to be random and reversible-jump MCMC is used to simulate the posterior distribution. However, some parameters of the OU processes defined for the regimes, namely α and σ , are made common for all regimes, while θ can vary across the regimes. The ancestral value at the root X_0 is also set to be the same as one of the θ values. Another method [9] uses Hamiltonian Monte Carlo to simulate the posterior distribution of the OU model for multivariate observations at the tips, but not allowing for different regimes on the tree. While we assume that the regimes are fixed and the value at the tips to be univariate, we allow more flexibility in defining the models by allowing each regime to have either BM or OU process with complete parameters. The only common parameter for all regimes is the ancestral value at the root X_0 . We also implement a Monte Carlo algorithm that is based on importance sampling, which could be easily parallelized since it involves a lot of independent calculations.

2 Methods

We begin this section by explaining the procedures behind the method that we implemented, starting from the posterior sampling algorithm and the mechanism to evaluate the model. We proceed by explaining the setup for simulation study to assess the performance of our method in terms of parameter inference and model evaluation. Lastly, we describe the real-world data that we use and postulate different scenarios of evolution, to be tested using our method. Our software is available as an R [10] package `bgphy`, that is available to download from github.com/bayubeta/bgphy.

2.1 Bayesian inference of MGPM parameters

For convenience, the observation vector at the tips, $\mathbf{x} = (x_1, x_2, \dots, x_n)^\top$, is assumed to take values from \mathbb{R}^n . Since the observations are generally positive-valued, a one-to-one transformation to \mathbb{R}^n using the log function is commonly used before the inference procedure.

We implement a procedure that consists of multiple steps to simulate the posterior distribution of Θ given an MGPM \mathbf{M} with K regimes. First, we define the prior distribution of Θ by defining a prior distribution for each parameter individually, as explained in the Equation 5. The choices of different prior distributions are available in the `bgphy` package.

To make things easier for the Monte Carlo algorithm that involves sampling from the multivariate normal distribution, we transform the prior distribution into a transformed prior distribution that takes values from \mathbb{R}^d , where $d = \dim(\Theta)$. Since the parameters are assumed to be pairwise independent, we use a class of well-behaved and one-to-one functions [11] to transform the parameters individually. Let $g : \mathcal{S}_\Theta \rightarrow \mathbb{R}^d$, where \mathcal{S}_Θ is the original space of parameters Θ .

With a slight abuse of notations, we keep the symbol Θ for the transformed prior, but we remind the reader that we are working on the transformed, unbounded space of \mathbb{R}^d that is the result of transforming the original Θ space by the function g , i.e., $\Theta \leftarrow g(\Theta)$.

The posterior sampling scheme follows the Population Monte Carlo (PMC, [12]) procedure, which involves several schemes of importance sampling and resampling. The PMC scheme is chosen because it is an improvement on the standard importance sampling scheme which heavily depends on the choice of the proposal distribution. On the other hand, it can be seen as a specific case of a more advanced Sequential Monte Carlo sampler scheme [13], but requires less likelihood calculations which can be relatively expensive because of the phylogenetic relations of the observations. In this manner, PMC is a good trade-off between inference quality and speed.

We adapt the PMC algorithm by using Laplace’s approximation as the initial generating distribution and local Gaussian distributions as the generating distributions after a resampling step.

Specifically, we begin by drawing samples from \mathbb{R}^d ,

$$\Theta_1^{(1)}, \dots, \Theta_S^{(1)} \stackrel{iid}{\sim} \mathcal{MVN} \left(\Theta \mid \hat{\Theta}, (-\hat{\mathbf{H}}_{\Theta})^{-1} \right), \quad (6)$$

with density function $q(\Theta)$, which is a multivariate normal distribution with mean that is located at the posterior mode $\hat{\Theta}$ and has the inverse of the negative of the approximated Hessian matrix around the posterior mode as the covariance. In `bgphy`, the mode search and the Hessian calculation are done numerically using the `optim R` function. We then calculate the (normalized) weights of the drawn samples by

$$w_i^{(1)} = \frac{\tilde{w}(\Theta_i^{(1)})}{\sum_{j=1}^S \tilde{w}(\Theta_j^{(1)})}, \text{ where } \tilde{w}(\Theta_i^{(1)}) = \frac{\mathcal{L}(\Theta_i^{(1)})p(\Theta_i^{(1)})}{q(\Theta_i^{(1)})}. \quad (7)$$

In the next step, a resampling step is done by creating a new set of samples from the old ones. We do this by choosing randomly with replacements from $\Theta_1^{(1)}, \dots, \Theta_S^{(1)}$ with probabilities $w_1^{(1)}, \dots, w_S^{(1)}$. To put it another way, we sample the indices

$$a_i, \dots, a_S \stackrel{iid}{\sim} \text{Categorical}(\{w_1^{(1)}, \dots, w_S^{(1)}\}), \quad (8)$$

and use them to define $\Theta_1^{(2)}, \dots, \Theta_S^{(2)}$, where $\Theta_i^{(2)} = \Theta_{a_i}^{(1)}$. This step is important in throwing away samples that have low or close-to-zero weights, which indicates that they are far from the high posterior density area.

We proceed by drawing new samples $\Theta_1, \dots, \Theta_S$, where

$$\Theta_i \sim \mathcal{MVN} \left(\Theta \mid \Theta_i^{(2)}, \Sigma_{\Theta^{(2)}} \right). \quad (9)$$

That is, for each sample $\Theta_i^{(2)}$, we draw a new sample from a multivariate normal distribution centered around $\Theta_i^{(2)}$, while the covariance matrix can be made common for all $i = 1, \dots, S$. We set $\Sigma_{\Theta^{(2)}}$ to be a diagonal matrix where $\Sigma_{\Theta^{(2)}} = \frac{1}{S} \text{diag}(\hat{\sigma}_1^2, \dots, \hat{\sigma}_d^2)$, i.e., $\frac{1}{S}$ times a diagonal matrix where the element in the j -th row and column is the sample variance of the j -th dimension of $\Theta^{(2)}$ from all S samples, $1 \leq j \leq d$.

Finally, we calculate the weights for the new sample with a similar procedure as in Equation 7, but we adjust the density function q , such that

$$w_i = \frac{w^*(\Theta_i)}{\sum_{j=1}^S w^*(\Theta_j)}, \text{ where, } w^*(\Theta_i) = \frac{\mathcal{L}(\Theta_i)p(\Theta_i)}{q_i(\Theta_i)}, \quad (10)$$

where q_i is the density function of the multivariate normal distribution that generates Θ_i . The pseudo-code for the posterior sampling scheme is illustrated by Algorithm 1.

The output of this sampling procedure is a set of pairs of parameter values and their weights, $\{\Theta_1, w_1\}, \dots, \{\Theta_S, w_S\}$, which can be directly used to approximate integrals that arise when calculating expected values of functions with respect to the posterior distribution:

$$\mathbb{E}_{\Theta|\mathbf{x}}[h(\Theta)] = \int h(\Theta)p(\Theta|\mathbf{x})d\Theta \approx \sum_{i=1}^S h(\Theta_i)w_i. \quad (11)$$

As an example, $h(\Theta) = \Theta$ results into the expected value of the posterior distribution, $\mathbb{E}_{\Theta|\mathbf{x}}[\Theta]$, that can be approximated by the sum $\sum_{i=1}^S \Theta_i w_i$.

2.2 Model evaluation and comparison

The conventional method to evaluate a model in a Bayesian setting is to use Bayes factor, where the ratio of marginal likelihood terms of competing models \mathbf{M}_0 and \mathbf{M}_1 ,

$$BF_{1,0} = \frac{p(\mathbf{x}|\mathbf{M}_1)}{p(\mathbf{x}|\mathbf{M}_0)}, \quad (12)$$

is calculated. This is viewed as a measure of evidence found in the observed data for one statistical model against another [14]. Each term on the ratio above can be obtained by computing the integral

$$p(\mathbf{x}|\mathbf{M}_i) = \int p(\mathbf{x}|\Theta_i, \mathbf{M}_i)p(\Theta_i|\mathbf{M}_i)d\Theta_i, \quad (13)$$

for $i = 0, 1$, which implicitly penalizes model complexity, since a more constrained model is preferred when it results in a similar fit to the observations as the more complex model [15].

However, Bayes factor is not without its shortcomings. The Bayes factor in Equation 12 alone is not enough to determine which model is more likely to be true

Algorithm 1 Posterior sampling scheme

Require:

- Phylogenetic tree \mathcal{T} .
- Observed data at the tips, \mathbf{x} .
- An MGPM \mathbf{M} , with parameters set Θ , $\dim(\Theta) = d$, consisting of a regime configurations with K regimes.
- Prior distribution $p(\Theta)$.
- Number of Monte Carlo samples, S .
- Transformation function, g .

Output: Pairs of samples from the parameter space and their weights, $\{\Theta_1, w_1\}, \dots, \{\Theta_S, w_S\}$.

Begin:

- 1: Transform Θ and $p(\Theta)$ g .
 - 2: $\Theta_1^{(1)}, \dots, \Theta_S^{(1)} \stackrel{iid}{\sim} q(\Theta) = \mathcal{M}\mathcal{V}\mathcal{N}\left(\Theta \mid \hat{\Theta}, (-\hat{\mathbf{H}}_{\hat{\Theta}})^{-1}\right)$
 - 3: **for** $i = 1, \dots, S$ **do**
 - 4: $w_i^{(1)} = \frac{\tilde{w}(\Theta_i^{(1)})}{\sum_{j=1}^S \tilde{w}(\Theta_j^{(1)})}$, where $\tilde{w}(\Theta_i^{(1)}) = \frac{\mathcal{L}(\Theta_i^{(1)})p(\Theta_i^{(1)})}{q(\Theta_i^{(1)})}$.
 - 5: **end for**
 - 6: **for** $i = 1, \dots, S$ **do**
 - 7: $a_i \sim \text{Cat}(\{w_1^{(1)}, \dots, w_S^{(1)}\})$
 - 8: $\Theta_i^{(2)} = \Theta_{a_i}^{(1)}$
 - 9: **end for**
 - 10: $\Sigma_{\Theta^{(2)}} = \frac{1}{S} \text{diag}(\hat{\sigma}_1^2, \dots, \hat{\sigma}_d^2)$, where $\hat{\sigma}_j^2$ is the sample variance of the j -th dimension of $\Theta^{(2)}$ from all S samples, $1 \leq j \leq d$.
 - 11: **for** $i = 1, \dots, S$ **do**
 - 12: $\Theta_i \sim q_i(\Theta) = \mathcal{M}\mathcal{V}\mathcal{N}\left(\Theta \mid \Theta_i^{(2)}, \Sigma_{\Theta^{(2)}}\right)$
 - 13: **end for**
 - 14: **for** $i = 1, \dots, S$ **do**
 - 15: $w_i = \frac{w^*(\Theta_i)}{\sum_{j=1}^S w^*(\Theta_j)}$, where $w^*(\Theta_i) = \frac{\mathcal{L}(\Theta_i)p(\Theta_i)}{q_i(\Theta_i)}$.
 - 16: **end for**
 - 17: Transform back $\{\Theta_i\}_{i=1}^S$ using g^{-1} .
-

given the observed data, which is done by calculating the posterior odds,

$$\frac{p(\mathbf{M}_1|\mathbf{x})}{p(\mathbf{M}_0|\mathbf{x})} = \frac{p(\mathbf{x}|\mathbf{M}_1)}{p(\mathbf{x}|\mathbf{M}_0)} \times \frac{p(\mathbf{M}_1)}{p(\mathbf{M}_0)} \quad (14)$$

$$= BF_{1,0} \times \frac{p(\mathbf{M}_1)}{p(\mathbf{M}_0)}, \quad (15)$$

where the term $p(\mathbf{M}_1)/p(\mathbf{M}_0)$ is the prior odds. By calculating the Equation 12 directly, we assume that $p(\mathbf{M}_1) = p(\mathbf{M}_0)$. Therefore, the threshold on deciding if a

model can be considered more plausible or not given the observed data depends on the prior beliefs on the models, which are not easy to determine. Moreover, additional computations need to be done to obtain the integral in Equation 13, which is not usually available in closed-form. On top of that, the marginal likelihood can be sensitive to the choice of prior over the parameters Θ_i (see [16] and [17]).

Another way to evaluate the fitness of a model to the observed data is by comparing the data replicated under the model and the observed data. In principle, a model that is more plausible to explain the data-generating process should be able to replicate data at the tips that are close to the observed data. To do this, we compare the posterior predictive distribution with the observed data [18].

In our problem, the density of the posterior predictive distribution can be formulated as

$$p(\tilde{\mathbf{x}}|\mathbf{x}) = \int p(\tilde{\mathbf{x}}|\Theta)p(\Theta|\mathbf{x})d\Theta, \quad (16)$$

i.e., it is a weighted average of the likelihood function $\mathcal{L}(\Theta) = p(\tilde{\mathbf{x}}|\Theta)$ over the posterior distribution $\Theta|\mathbf{x}$.

We adapt the posterior predictive loss formulation [19] to our problem as follows:

$$\begin{aligned} & \|\mathbf{x} - \mathbb{E}[\tilde{\mathbf{x}}|\mathbf{x}]\|_2 + \text{tr}(\text{Cov}(\tilde{\mathbf{x}}|\mathbf{x})) \\ &= \sum_{i=1}^n (x_i - \mathbb{E}[\tilde{x}_i|\mathbf{x}])^2 + \sum_{i=1}^n \text{Var}(\tilde{x}_i|\mathbf{x}), \end{aligned} \quad (17)$$

where x_i is the observed data point at tip i and $\tilde{x}_i|\mathbf{x}$ is the marginal posterior predictive distribution at tip i .

The formula above consists of two terms. The first term is the sum of squared errors (SSE) to collect the discrepancies between the observed data at tip i and the expected value of marginal posterior predictive distribution at tip i . Thus, a lower SSE score indicates that the posterior predictive distribution is closer to the observed data. The second term is the sum of variances of the marginal posterior predictive distribution from all tips. Under a model with a lot of parameters, the SSE would be lower but the sum of variances would be higher since the replicated data could be more diverse. Therefore, the sum of variances term acts as a penalizing term for the model complexity.

The posterior predictive loss on Equation 2.2 relies on the posterior predictive distribution $\tilde{\mathbf{x}}|\mathbf{x}$, which is not analytically available. However, we can still estimate it by simulating samples from the posterior predictive distribution. We do this in two steps: first is to sample parameter values from the posterior distribution, and second is to simulate observations at the tips by running the MGPM with the posterior samples. By using the results from subsection 2.1, samples from the posterior distribution can be drawn by performing a resampling process over the posterior parameters $\Theta_i, \dots, \Theta_S$. Algorithm 2 shows the pseudo-code of this posterior predictive sampling process.

The simulated observations from the posterior predictive distribution, $\tilde{\mathbf{x}}^{(1)}, \dots, \tilde{\mathbf{x}}^{(S)}$, from algorithm 2 can be used to estimate equation . Let

Algorithm 2 Posterior predictive sampling scheme

Require:

- Phylogenetic tree \mathcal{T} .
- An MGPM \mathbf{M} consisting of a regime configurations with K regimes.
- Number of Monte Carlo samples, S_p .
- Parameters and weights from Algorithm 1, $\{\Theta_1, w_1\}, \dots, \{\Theta_S, w_S\}$.

Output: Samples from the posterior predictive distribution, $\tilde{\mathbf{x}}_1, \dots, \tilde{\mathbf{x}}_{S_p}$.

Begin:

- 1: **for** $i = 1, \dots, S_p$ **do**
Sample from posterior distribution:
 - 2: $a_i \sim \text{Cat}(\{w_1, \dots, w_S\})$
 - 3: $\Theta_i^* = \Theta_{a_i}$
Simulate observations at the tips:
 - 4: $\tilde{\mathbf{x}}^{(i)} \sim \mathbf{M}(\Theta_i^*, \mathcal{T})$
 - 5: **end for**
-

$\tilde{\mathbf{x}}^{(i)} = (\tilde{x}_1^{(i)}, \tilde{x}_2^{(i)}, \dots, \tilde{x}_n^{(i)})^\top$. Then, the estimated posterior predictive loss is

$$\text{post. pred. loss} = \sum_{i=1}^n (x_i - \tilde{m}_i)^2 + \sum_{i=1}^n \tilde{s}_i^2, \quad (18)$$

where

$$\tilde{m}_i = \frac{1}{S_p} \sum_{j=1}^{S_p} \tilde{x}_i^{(j)} \quad \text{and} \quad \tilde{s}_i^2 = \frac{1}{S_p - 1} \sum_{j=1}^{S_p} (\tilde{x}_i^{(j)} - \tilde{m}_i)^2. \quad (19)$$

Respectively, \tilde{m}_i and \tilde{s}_i^2 are the i -th element of the sample mean and the i -th element of the diagonal of the sample variance-covariance matrix from all the simulated observations.

2.3 Method assessment

2.3.1 Simulation study

Parameter estimation. To see the capability of our method in terms of parameter estimation, we perform a study that is based on simulated data. We use the post-processed phylogenetic tree of *Anolis* lizards [20, 21] which has a unit height and simulated data at the tips of the tree. As the MGPM, we create a scenario where there are two regimes on the tree: *Ancestral*, which has parameters $\alpha_1 = 2$, $\theta_1 = 2$, and $\sigma_1 = 1$, and R_1 with parameters $\alpha_2 = 5$, $\theta_2 = 0$, and $\sigma_2 = 0.5$. The ancestral value at the root is set to be $X_0 = 0$. The regimes configuration on the tree and an example of the process to simulate the observations at the tips can be seen from Figure 2.

The priors for the parameters are set the same depending on their space. We put the half-normal prior with a scale parameter $\sigma = 10$ for the positive parameters, $\alpha_1, \sigma_1, \alpha_2$, and σ_2 . For parameters that can take values from \mathbb{R} , X_0, θ_1 , and θ_2 , we chose the normal distribution with $\mu = 10$ and $\sigma^2 = 100$.

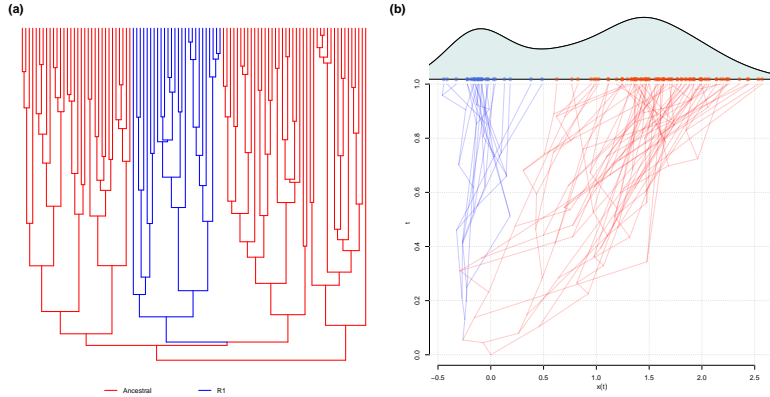


Fig. 2 (a) Regimes configuration on the phylogenetic tree. (b) An illustration of the process to simulate observations at the tips by simulating values in the internal nodes of the tree.

Using this setup, we simulated 100 sets of observations at the tips. For each simulated set of observations, we inferred the posterior parameters and compared them with the true parameter values. As a comparison, we also ran the maximum likelihood calculation given each set of observations using `PCMFit` [3]. Because of the random initialization for the maximum likelihood procedure and the complicated likelihood surface, we performed 100 maximum likelihood runs for each set of observations and pick a set of parameters that has the highest log-likelihood. We also restricted the search space to $[0, 100]$ for positive parameters (α 's and σ 's) and $[-200, 200]$ for X_0 and θ 's.

For both posterior and maximum likelihood inference, we assume that we know exactly the regimes configuration and the type of model in each regime (OU model).

Model evaluation. In the next part of the simulation study, we wanted to assess the model selection aspect of our method. Using the same phylogenetic tree for parameter estimation study, we defined three different MGPMs with increasing complexity, \mathbf{M}_1 , \mathbf{M}_2 , and \mathbf{M}_3 . \mathbf{M}_1 contains only one regime called *Ancestral*. In \mathbf{M}_2 , there are two OU regimes called *Ancestral* and *R1*, while \mathbf{M}_3 contains four OU regimes, which are *Ancestral*, *R1*, *R2*, and *R3*. All MGPMs start from ancestral value X_0 . The full list of true parameters for each MGPM and their configuration on the tree can be seen on Table 1 and Figure 3.

For each MGPM \mathbf{M}_1 , \mathbf{M}_2 , and \mathbf{M}_3 , we simulated 100 sets of observations at the tips. Then, for each set of simulated observations, we assumed the configurations and models in \mathbf{M}_1 , \mathbf{M}_2 , and \mathbf{M}_3 (without the true parameters) as the three different models of evolution, and find the posterior distributions of the parameters, given the set of observations and the assumed model. Particularly, let $\mathbf{x}_i^{(j)}$ be the j -th simulated observations from the MGPM \mathbf{M}_i . Then, we inferred the posterior distributions $p(\Theta_k | \mathbf{x}_i^{(j)}, \mathbf{M}_k)$, for $k = 1, 2, 3$, where Θ_k is the set of parameters of the assumed model \mathbf{M}_k . From each posterior inference, we computed the posterior predictive loss score, and compared them among different scenarios.

Table 1 List of true parameters in all regimes for M_1 , M_2 , and M_3 . The parameter for ancestral value at the root, X_0 , is set to the *Global* regime as it is shared among all other regimes.

MGPM	Regime	Model	True parameters
M_1	Global	-	$X_0 = 0$
	Ancestral	OU	$\alpha = 2, \theta = 2, \sigma = 1$
M_2	Global	-	$X_0 = 0$
	Ancestral	OU	$\alpha = 2, \theta = 2, \sigma = 2$
	R1	OU	$\alpha = 1, \theta = -2, \sigma = 1$
M_3	Global	-	$X_0 = 0$
	Ancestral	OU	$\alpha = 3, \theta = 2, \sigma = 2$
	R1	OU	$\alpha = 2, \theta = 1, \sigma = 1$
	R2	OU	$\alpha = 2, \theta = -1, \sigma = 1$
	R3	OU	$\alpha = 3, \theta = -2, \sigma = 2$

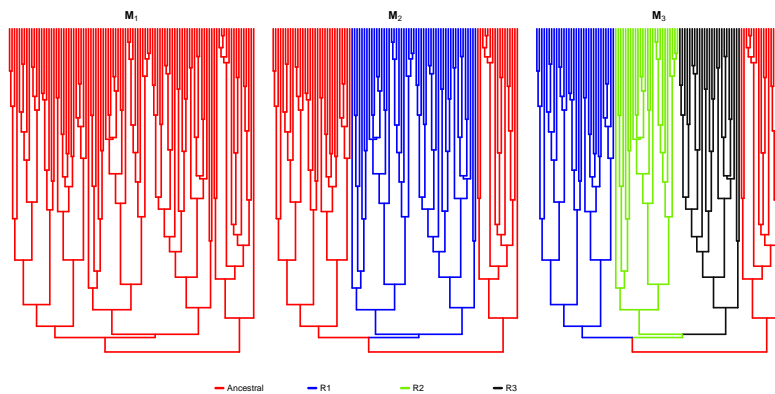


Fig. 3 Configurations of evolutionary regimes for the MGPM M_1 , M_2 , and M_3 . For M_1 , there is only a single, global regime that is the same as the root node. The tree is split into two regimes for M_2 , and four regimes for M_3 .

2.3.2 Real-world data

We used our method to study the evolutionary process of antler size across the deer (family Cervidae) phylogeny [5]. We chose the trait posterior skull length (PSL) as the proxy for the antler size and hypothesized three different scenarios of evolution of the antlers. First, the antler size is assumed to evolve under the same process regardless of their position in the phylogenetic tree. Second, we assume that the antlers of the old-world and the new-world deer species evolved under different processes, hence the tree is split into two regimes. Third, we assume that the antler types, palmated (Palm), main beamed (MB), and bifurcated, have different evolutionary processes, and model the most common type, MB as the ancestral regime while mapping the regimes for palmated and bifurcated types onto terminals or clades where they are observed as tip data unequivocally. We proceed by denoting the MGPM for the first, second, and the

third scenario as \mathbf{M}_a , \mathbf{M}_b , and \mathbf{M}_c , respectively. The regimes configurations of \mathbf{M}_a , \mathbf{M}_b , and \mathbf{M}_c on the tree and the observed data at the tips can be seen on Figure 4.

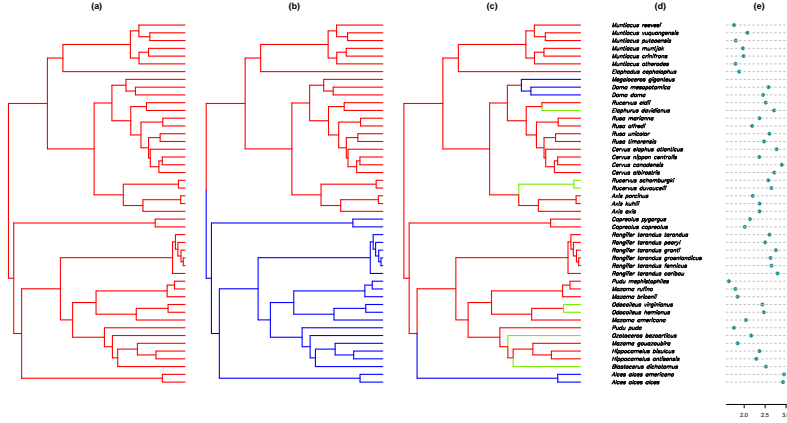


Fig. 4 Different scenarios of regimes configuration on the antlers phylogeny. In **(a)**, there is only one regime for the whole tree. In **(b)**, the red regime denotes the old-world deer while the blue regime denotes the new-world deer. In the third scenario, **c**, the tree is split into three regimes based on the antler shape: main beamed (MB, red), palmated (Palm, blue), and bifurcated (green). Subplot **(d)** lists the taxa names found in the tree, while subplot **(e)** shows the value of log of posterior skull length (PSL) for each taxon.

For all regimes, we assume an OU process with parameters α , θ , and σ , unique to that regime, and X_0 that is shared among all regimes in one scenario. The prior distribution is set the same for all α 's and σ 's, that is half-normal distribution with a scale parameter $\sigma = 20$. For all θ 's and X_0 's, the prior distribution is a normal distribution with mean $\mu = 0$ and variance $\sigma^2 = 100$. The full list of parameters and their prior distributions for each MGPM are shown on Table 2. We compared the fit of each scenario to the observed data, measured by the posterior predictive loss score.

Table 2 List of models on the regimes of \mathbf{M}_a , \mathbf{M}_b , and \mathbf{M}_c , with their parameters and priors. The parameter for ancestral value at the root, X_0 , is set to the *Global* regime as it is shared among all other regimes.

MGPM	Regime	Model	Parameters and priors
\mathbf{M}_a	Global	-	$X_0 \sim \mathcal{N}(\mu = 0, \sigma^2 = 100)$
	Ancestral	OU	$\alpha \sim \text{Half-}\mathcal{N}(\sigma = 20)$, $\theta \sim \mathcal{N}(\mu = 0, \sigma^2 = 100)$, $\sigma \sim \text{Half-}\mathcal{N}(\sigma = 20)$
\mathbf{M}_b	Global	-	$X_0 \sim \mathcal{N}(\mu = 0, \sigma^2 = 100)$
	Old-world	OU	$\alpha_1 \sim \text{Half-}\mathcal{N}(\sigma = 20)$, $\theta_1 \sim \mathcal{N}(\mu = 0, \sigma^2 = 100)$, $\sigma_1 \sim \text{Half-}\mathcal{N}(\sigma = 20)$
	New-world	OU	$\alpha_2 \sim \text{Half-}\mathcal{N}(\sigma = 20)$, $\theta_2 \sim \mathcal{N}(\mu = 0, \sigma^2 = 100)$, $\sigma_2 \sim \text{Half-}\mathcal{N}(\sigma = 20)$
\mathbf{M}_c	Global	-	$X_0 \sim \mathcal{N}(\mu = 0, \sigma^2 = 100)$
	MB	OU	$\alpha_1 \sim \text{Half-}\mathcal{N}(\sigma = 20)$, $\theta_1 \sim \mathcal{N}(\mu = 0, \sigma^2 = 100)$, $\sigma_1 \sim \text{Half-}\mathcal{N}(\sigma = 20)$
	Palm	OU	$\alpha_2 \sim \text{Half-}\mathcal{N}(\sigma = 20)$, $\theta_2 \sim \mathcal{N}(\mu = 0, \sigma^2 = 100)$, $\sigma_2 \sim \text{Half-}\mathcal{N}(\sigma = 20)$
	Bifurcated	OU	$\alpha_3 \sim \text{Half-}\mathcal{N}(\sigma = 20)$, $\theta_3 \sim \mathcal{N}(\mu = 0, \sigma^2 = 100)$, $\sigma_3 \sim \text{Half-}\mathcal{N}(\sigma = 20)$

3 Results

3.1 Simulation study

Parameter estimation. Figure 5a shows the boxplots of median of the marginal posterior distributions and the boxplots of the maximum likelihood estimates, compared to the true parameter values. The medians of the marginal posterior distributions for θ_1 and θ_2 are the closest to the true values, followed by σ_1 and σ_2 . Although the medians of X_0 are mostly around the true values, the medians of the rate parameters α_1 and α_2 are larger than the true values.

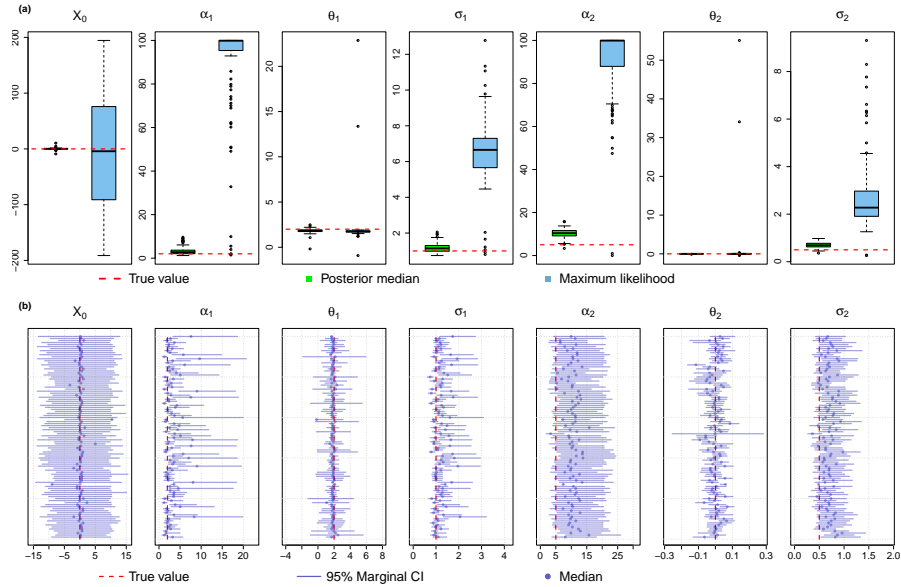


Fig. 5 (a) Boxplots of 100 posterior medians (light green) and maximum likelihood estimates (light blue) compared to the true parameter values (red dashed lines). (b) The 95% equal-tailed credible intervals of the marginal posterior distribution. There are 100 intervals shown for each parameter, along with the medians.

We can also see the posterior distribution of parameters through their 95% equal-tailed credible intervals, which is shown in Figure 5b. Even though the medians of the marginal posterior distribution for some parameters are higher than the true values, i.e., α_1 , α_2 , σ_1 , and σ_2 , most of the time the true values are still included in the credible intervals.

Compared to the maximum likelihood estimates, the posterior medians are in general closer to the true values. In some cases where the medians are larger than the true values, i.e., α_1 , α_2 , σ_1 , and σ_2 , the maximum likelihood estimates are much higher. This is due to the fact that the prior distributions, even though they are weakly informative, put lower probabilities on unrealistic parameter values, e.g., high α or σ . This

could result in posterior distributions that are more confined into more realistic parameter values, and this might be a remedy to one of the problems of maximum likelihood based inference for PCMs, that is, large estimates of α and σ (see, e.g., [22]).

Moreover, maximum likelihood estimates are done by performing optimization routines on the likelihood space, which could be multimodal or even flat. Hence, the optimization algorithm could easily be stuck at a local maximum.

Model evaluation. The posterior predictive loss values of MGPMs \mathbf{M}_1 , \mathbf{M}_2 , and \mathbf{M}_3 , given the observed data simulated by each of them can be seen on Figure 6. When the observations are simulated from \mathbf{M}_1 , the three models are comparable in terms of their posterior predictive loss scores. Once we observed a more complicated set of observations simulated from \mathbf{M}_2 , we can see that the models \mathbf{M}_2 and \mathbf{M}_3 have lower scores than \mathbf{M}_1 . Finally, \mathbf{M}_3 has the lowest scores when the observations are generated by \mathbf{M}_3 .

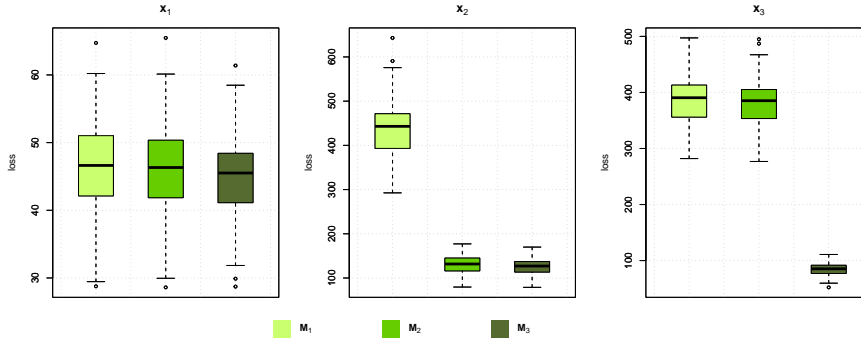


Fig. 6 Boxplots of posterior predictive loss scores. The left-hand-side shows the boxplots for posterior predictive loss scores from MGPMs \mathbf{M}_1 , \mathbf{M}_2 , and \mathbf{M}_3 , given that the observations are simulated from \mathbf{M}_1 . Similarly, the center and the right-hand-side plot shows posterior predictive loss scores when the observations are simulated from \mathbf{M}_2 and \mathbf{M}_3 , respectively.

3.2 Real-world data

The comparison of posterior predictive distributions for MGPMs \mathbf{M}_a , \mathbf{M}_b , and \mathbf{M}_c can be seen on Figure 7. However, \mathbf{M}_b , the MGPM in which the regimes are based on old-world and new-world deer, has a higher posterior predictive loss score than \mathbf{M}_a , which assumes the same OU process throughout the whole tree. This suggests that the regimes configurations based on taxonomic definitions of old-world and new-world deer does not result in a model that can better explain the observed data than the single OU model.

By contrast, the MGPM \mathbf{M}_c has a lower score than the other two MGPMs, which does not seem to be obvious from the posterior predictive plots. However, its 95% posterior predictive density region is slightly shifted to the higher log PSL value, which is closer to the mode of the density of the observed data. This indicates that the simulated observations from the posterior predictive distributions of \mathbf{M}_c are closer to the true observed data at the tips.

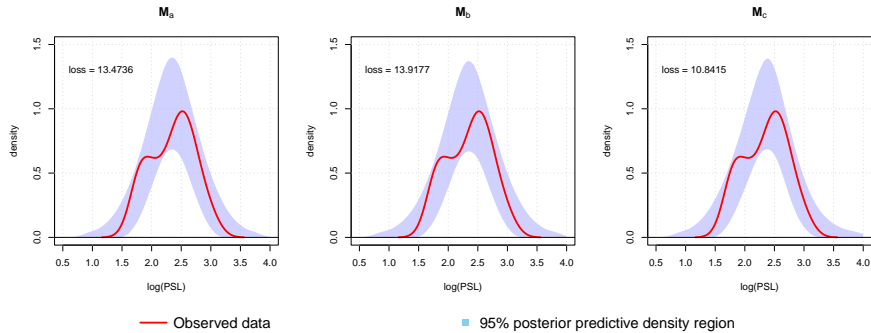


Fig. 7 From left to right: Density of the observed data compared to the density of the simulated data from the posterior predictive distribution assuming M_a , M_b , or M_c as the model of evolution.

4 Discussion

Simulation studies showed that our method can do parameter inference based on the posterior distribution properly. The posterior distribution of MGPM parameters inferred using our method is in general closer to the true parameters that generated the simulated data, compared to the maximum likelihood estimates. Even though this is not an exactly equivalent comparison, since we compare a Bayesian and a maximum likelihood method, this shows that the PMC algorithm that we implemented to do the Bayesian inference managed to capture the high posterior density area, which is mainly driven by the likelihood term since we used weakly informative priors.

The advantage of using prior distribution is apparent in preventing the inference to explore parts of the parameter space that result in unrealistic parameter values. In spite of that, defining a proper prior distribution can be challenging, especially when there is a lot of uncertainty around it since the observed data are often only available at the tips. Additionally, there is still issues model identifiability, which is only alleviated partly by the prior distribution. Inclusion of fossil data could further ease this problem, specifically in breaking down symmetry between different models or regimes [23].

Evidently, the posterior predictive loss is a good measure on how the hypothesized MGPM agrees with the observations. This demonstrates that the method is capable of selecting the more appropriate model for the more complicated observations. For simpler observations, the posterior predictive loss scores between all models are not significantly distinguishable. This could be interpreted as all models explain the generative process of the observations just as well. If one follows Occam's razor principle then a simpler model may be preferred.

It should be noted that in the simulation study for parameter estimation, we always assumed that we know exactly the true regimes and their true models, both for the posterior and maximum likelihood setting (without the true parameters). This is done to emulate the condition where there is no model mismatch. Hence, the conclusions drawn from the experiment only concern the parameter inference capability. In the

model evaluation study, we included one true MGPM among the three hypotheses, which is an ideal condition where we have the true model as one of our hypotheses.

We illustrate how our method can be used to test several evolutionary hypotheses in a real world setting. We showed how an MGPM with multiple regimes does not necessarily result in a better fit to the observed data than using a single process on the whole tree. However, a regime configuration based on a more natural classification of traits, i.e., shape of the antlers, results in an MGPM that is more plausible in explaining the process that generated observed data.

We would like to underline that we do not write that we have found the "true" model, since it might not be within our considered hypotheses. This is shown in 3.2 where all three hypotheses resulted in posterior predictive distributions that are unimodal, contrary to the empirical distribution of the data which is bimodal. What we are interested in is comparing multiple models that could explain the data-generating process. A better (lower) posterior predictive loss score could indicate that a model explains the data-generating process better, and hence captures some key properties in the data. However, one could easily construct such an overly complex model that excels in terms of posterior predictive loss score. Hence, each model under consideration should correspond to a carefully thought-through hypothesis so that the indicated model is interpretable (but this is essentially a warning common to any model selection procedure).

An obvious limitation of our method lies in the assumptions of fixed tree and fixed regimes. Since the tree itself is a result of inference from molecular sequences, it would make more sense to include the uncertainties regarding the tree itself, by including the molecular data. This has been done previously in multiple studies (see, e.g., [9, 24, 25]). On top of that, while the method is built on PCMBase engine that utilizes fast likelihood calculation, the posterior inference is implemented in pure R which leaves a room for improvement in terms of speed.

5 Conclusion

In this work, we implemented a Bayesian inference method for mixed Gaussian phylogenetic models, a class of models for PCMs from the \mathcal{G}_{LInv} family of evolutionary processes. This offers a flexibility to have model with distinct processes with their own parameters on different parts of a phylogenetic tree. This method also provides the possibility on setting more biologically-informed priors on the parameters.

We demonstrated how prior information can be incorporated into an MGPM, and how the method can appropriately infer the posterior distribution. Moreover, the method is able to evaluate model fit and compare between several competing hypotheses through a measure of similarity between the observations and the posterior predictive distribution.

Implementation into the real-world data shows that our method can be used to compare different scenarios of evolution that resulted in the observed data from different taxa that share a evolutionary history.

The natural extension of our method would include multivariate traits that can interact and affect each other throughout their evolution. This extends to the need

for a more efficient sampling algorithm to sample from high-dimensional posterior distributions that can result from high-dimensional traits, that could possibly include molecular data.

Conflict of interests. The authors declare no conflict of interests.

Acknowledgements. The authors are supported by the ELLIIT Call C grant: Developing core-technologies for tree-based models. The authors would like to thank Niklas Wahlberg, Masahito Tsuboi, and Sridhar Halali for the valuable discussions.

References

- [1] Felsenstein, J.: Phylogenies and the comparative method. *The American Naturalist* **125**(1), 1–15 (1985)
- [2] Hansen, T.F.: Stabilizing selection and the comparative analysis of adaptation. *Evolution* **51**(5), 1341–1351 (1997)
- [3] Mitov, V., Bartoszek, K., Stadler, T.: Automatic generation of evolutionary hypotheses using mixed Gaussian phylogenetic models. *Proceedings of the National Academy of Sciences* **116**(34), 16921–16926 (2019)
- [4] Mitov, V., Bartoszek, K., Asimomitis, G., Stadler, T.: Fast likelihood calculation for multivariate Gaussian phylogenetic models with shifts. *Theoretical Population Biology* **131**, 66–78 (2020)
- [5] Tsuboi, M., Kopperud, B.T., Matschiner, M., Grabowski, M., Syrowatka, C., Pélabon, C., Hansen, T.F.: Antler allometry, the irish elk and gould revisited. *Evolutionary Biology* **51**(1), 149–165 (2024)
- [6] Uyeda, J.C., Harmon, L.J.: A novel Bayesian method for inferring and interpreting the dynamics of adaptive landscapes from phylogenetic comparative data. *Systematic biology* **63**(6), 902–918 (2014)
- [7] Ho, L.S.T., Ané, C.: Intrinsic inference difficulties for trait evolution with Ornstein–Uhlenbeck models. *Methods in Ecology and Evolution* **5**(11), 1133–1146 (2014)
- [8] Cornuault, J.: Bayesian analyses of comparative data with the Ornstein–Uhlenbeck model: potential pitfalls. *Systematic Biology* **71**(6), 1524–1540 (2022)
- [9] Bastide, P., Ho, L.S.T., Baele, G., Lemey, P., Suchard, M.A.: Efficient bayesian inference of general Gaussian models on large phylogenetic trees. *The Annals of Applied Statistics* **15**(2), 971–997 (2021)
- [10] R Core Team: R: A Language and Environment for Statistical Computing. R Foundation for Statistical Computing, Vienna, Austria (2021). R Foundation for Statistical Computing. <https://www.R-project.org/>

- [11] Stan Development Team: The Stan Core Library. Version 2.18.0 (2018). <http://mc-stan.org>
- [12] Cappé, O., Guillin, A., Marin, J.-M., Robert, C.P.: Population Monte Carlo. *Journal of Computational and Graphical Statistics* **13**(4), 907–929 (2004)
- [13] Del Moral, P., Doucet, A., Jasra, A.: Sequential monte carlo samplers. *Journal of the Royal Statistical Society Series B: Statistical Methodology* **68**(3), 411–436 (2006)
- [14] Kass, R.E., Raftery, A.E.: Bayes factors. *Journal of the american statistical association* **90**(430), 773–795 (1995)
- [15] Lotfi, S., Izmailov, P., Benton, G., Goldblum, M., Wilson, A.G.: Bayesian model selection, the marginal likelihood, and generalization. In: *International Conference on Machine Learning*, pp. 14223–14247 (2022). PMLR
- [16] Tendeiro, J.N., Kiers, H.A.: A review of issues about null hypothesis bayesian testing. *Psychological methods* **24**(6), 774 (2019)
- [17] Campbell, H., Gustafson, P.: Bayes factors and posterior estimation: Two sides of the very same coin. *The American Statistician* **77**(3), 248–258 (2023)
- [18] Gelman, A., Carlin, J., Stern, H., Dunson, D., Vehtari, A., Rubin, D.: *Bayesian Data Analysis*, 3rd ed edn. Chapman and Hall/CRC, United States (2013)
- [19] Hooten, M.B., Hobbs, N.T.: A guide to Bayesian model selection for ecologists. *Ecological monographs* **85**(1), 3–28 (2015)
- [20] Mahler, D.L., Ingram, T., Revell, L.J., Losos, J.B.: Exceptional convergence on the macroevolutionary landscape in island lizard radiations. *Science* **341**(6143), 292–295 (2013)
- [21] Bastide, P., Didier, G.: The Cauchy process on phylogenies: A tractable model for pulsed evolution. *Systematic Biology* **72**(6), 1296–1315 (2023)
- [22] Bartoszek, K., Tredgett Clarke, J., Fuentes-González, J., Mitov, V., Pienaar, J., Piwczyński, M., Puchalka, R., Spalik, K., Voje, K.L.: Fast mvslouch: Multivariate ornstein–uhlenbeck-based models of trait evolution on large phylogenies. *Methods in Ecology and Evolution* **15**(9), 1507–1515 (2024)
- [23] Bastide, P., Ané, C., Robin, S., Mariadassou, M.: Inference of adaptive shifts for multivariate correlated traits. *Systematic Biology* **67**(4), 662–680 (2018)
- [24] Zhang, R., Drummond, A.J., Mendes, F.K.: Fast bayesian inference of phylogenies from multiple continuous characters. *Systematic Biology* **73**(1), 102–124 (2024)
- [25] Gaboriau, T., Mendes, F.K., Joly, S., Silvestro, D., Salamin, N.: A multi-platform

package for the analysis of intra-and interspecific trait evolution. *Methods in Ecology and Evolution* **11**(11), 1439–1447 (2020)